

Inhibiting the Formation of $(\text{Au}_{1-x}\text{Ni}_x)\text{Sn}_4$ and Reducing the Consumption of Ni Metallization in Solder Joints

C.E. HO,¹ L.C. SHIAU,¹ and C.R. KAO^{1,2}

1.—Department of Chemical and Materials Engineering, National Central University, Chungli City, Taiwan. 2.—E-mail: kaocr@hotmail.com

The effects of adding a small amount of Cu into eutectic PbSn solder on the interfacial reaction between the solder and the Au/Ni/Cu metallization were studied. Solder balls of two different compositions, 37Pb-63Sn (wt.%) and 36.8Pb-62.7Sn-0.5Cu, were used. The Au layer ($1 \pm 0.2 \mu\text{m}$) and Ni layer ($7 \pm 1 \mu\text{m}$) in the Au/Ni/Cu metallization were deposited by electroplating. After reflow, the solder joints were aged at 160°C for times ranging from 0 h to 2,000 h. For solder joints without Cu added (37Pb-63Sn), a thick layer of $(\text{Au}_{1-x}\text{Ni}_x)\text{Sn}_4$ was deposited over the Ni_3Sn_4 layer after the aging. This thick layer of $(\text{Au}_{1-x}\text{Ni}_x)\text{Sn}_4$ can severely weaken the solder joints. However, the addition of 0.5wt.%Cu (36.8Pb-62.7Sn-0.5Cu) completely inhibited the deposition of the $(\text{Au}_{1-x}\text{Ni}_x)\text{Sn}_4$ layer. Only a layer of $(\text{Cu}_{1-p-q}\text{Au}_p\text{Ni}_q)_6\text{Sn}_5$ formed at the interface of the Cu-doped solder joints. Moreover, it was discovered that the formation of $(\text{Cu}_{1-p-q}\text{Au}_p\text{Ni}_q)_6\text{Sn}_5$ significantly reduced the consumption rate of the Ni layer. This reduction in Ni consumption suggests that a thinner Ni layer can be used in Cu-doped solder joints. Rationalizations for these effects are presented in this paper.

Key words: Solder, solder joint, Au/Ni/Cu metallization, intermetallic

INTRODUCTION

Reflow soldering is one of the major soldering approaches to produce solder joints. For the eutectic PbSn solder, the peak reflow temperature is generally $200\text{--}235^\circ\text{C}$, and the typical reflow time that the solder is in the molten state is $60\text{--}120$ sec. During reflow, solder melts and reacts with the solderable surface finish of the soldering pad. The Au/Ni/Cu tri-layer metallization is one of the most common surface finishes. The Au layer is for oxidation protection and is usually $0.2\text{--}1.0\text{-}\mu\text{m}$ thick when deposited by electroplating. The function of the Ni layer is to prevent the rapid reaction between the solder and the Cu layer, which is part of the internal conducting wiring of an electronic package. The reaction rate between molten PbSn solder and Cu is 100 times faster than that between PbSn solder and Ni.¹ Without the Ni layer as a diffusion barrier, rapid reaction between Sn and Cu occurs, and the Cu layer could be quickly consumed. The Ni layer in the ball-grid array (BGA) package is often deposited by electro-

plating and is about $5\text{--}10\text{-}\mu\text{m}$ thick. At 160°C , a $7\text{-}\mu\text{m}$ Ni layer is able to protect the Cu for about 2,500 h.² In flip-chip technology, however, the Ni layer is typically deposited by evaporation or sputtering and is only several thousand angstroms thick. The consumption rate of Ni then becomes a major concern in designing a flip-chip package.

During the very early stage of reflow, solder reacts with the Au layer to form AuSn_4 . The compound AuSn_4 would then detach itself from the interface. This reaction and subsequent detachment is very rapid. The time required for an $1\text{-}\mu\text{m}$ Au to disappear from the interface is less than 10 sec.³ After the Au layer disappears from the interface, Ni comes into contact with the molten solder and starts to react with the solder. According to Kulojärvi et al.,⁴ the consumption rate of Ni into eutectic PbSn solder was about $0.002 \mu\text{m}/\text{sec}$ at 220°C . Therefore, it can be roughly estimated that during a typical reflow (with the solder being molten for, say, 110 sec), $(0.002 \mu\text{m}/\text{sec}) \times (110 \text{ sec} - 10 \text{ sec}) = 0.2 \mu\text{m}$ of Ni will be consumed. This estimate represents an upper-limit approximation because the temperature of the molten solder does not stay as high as 220°C

(Received February 12, 2002; accepted May 29, 2002)

during the entire 110-sec reflow time, and a 110-sec reflow time is considered long for most applications. Comparing the value of $0.2\ \mu\text{m}$ with the Ni thickness in flip-chip packages, one must seriously consider the possibility of the Ni layer being completely consumed during the life cycle of an electronic product or even during the reflow process. The first objective of this study is to investigate the effect of adding Cu into the solder on the Ni consumption rate.

It was reported that a thick layer of $(\text{Au}_{1-x}\text{Ni}_x)\text{Sn}_4$ would deposit at the interface after a solder joint was subjected to solid-state aging at 100°C or higher for a few hundred hours.^{2,5-10} This thick layer of $(\text{Au}_{1-x}\text{Ni}_x)\text{Sn}_4$ can severely weaken the solder joints. Recently, it was shown that the addition of Cu to the solder could inhibit the deposition of $(\text{Au}_{1-x}\text{Ni}_x)\text{Sn}_4$.^{11,12} The second object of this study is to understand the mechanism of the inhibition.

EXPERIMENTAL PROCEDURE

The soldering pads used in this study had a diameter of $720\ \mu\text{m}$, but the outer rim of each pad was covered with the solder mask so that only the inner $600\text{-}\mu\text{m}$ diameter of the surface finish was exposed to the solder. The Au layer and Ni layer in the Au/Ni/Cu surface finish were deposited by electroplating and were $1 \pm 0.2\text{-}\mu\text{m}$ thick and $7 \pm 1\text{-}\mu\text{m}$ thick, respectively. Two types of solders were used: the PbSn eutectic (37Pb-63Sn) and an eutectic PbSn-based solder but with a small amount of Cu added (36.8Pb-62.7Sn-0.5Cu). The solder ball diameter was $750\ \mu\text{m}$, and the mass of each ball was 2 mg. In addition to reflowing the two types of solder on Au/Ni/Cu, the 37Pb-63Sn solder was also reflowed on solder pads that had only a layer of Ni over Cu (Ni/Cu). On these Ni/Cu pads, the Ni thickness is about the same as that in Au/Ni/Cu, but the Au layer was not plated. The exact thickness of Au as well as Ni for each substrate was measured from the neighboring pads that did not participate in the reaction.

For the reflow, the peak reflow temperature was fixed at 225°C . The reflow time over 183°C , the PbSn eutectic temperature, was 115 sec. After the reflow, substrates were then subjected to aging at 160°C for time up to 2,000 h. After the aging treatment, the solder joints were sectioned using a low-speed diamond saw and metallographically polished to reveal the interface and the internal microstructure of the solder joints. To reveal the cross-sectional microstructure, the samples were etched with a 5vol.%HCl in methanol for 10–15 sec. The etchant for the top-view micrographs was a 30vol.%HNO₃ aqueous solution. The etching time depended on the thickness of the solder over the interface. The thickness of the reaction products and the thickness of the remaining Ni layer were measured by using image analysis software. The thickness is defined as the total area of the phase divided by the linear length of the interface. The composition of each phase was de-

termined by using an electron microprobe analyzer (EPMA), operated at 20 keV. During the microprobe measurements, the detected x-ray lines were K_α , K_β , L_α , L_β , and L_γ for Cu, Ni, Au, Pb, and Sn, respectively. For x-ray diffraction (XRD) analysis, the Cu K_α radiation was used. A 200 keV transmission electron microscope (TEM) was also used to identify the structure of the reaction product.

RESULTS

Three types of interfacial reactions were carried out in this study: the reaction between 37Pb-63Sn and Au/Ni/Cu (experiment I), the reaction between 37Pb-63Sn and Ni/Cu (experiment II), and the reaction between 36.8Pb-62.7Sn-0.5Cu and Au/Ni/Cu (experiment III). In the following, the results, right after reflow, are presented and then the results after reflow and aging are presented.

Right after Reflow

After reflow, the entire $1\text{-}\mu\text{m}$ Au layer disappeared from the interface, and the Ni was exposed to the solder in experiment I. The Au atoms, amounting to about 0.4 wt.% of the solder, formed many $(\text{Au}_{1-x}\text{Ni}_x)\text{Sn}_4$ particles distributed evenly throughout the solder joint.^{3,8} At the interface, Ni reacted with Sn to form a layer of Ni_3Sn_4 , as shown in Fig. 1a. Figure 1b is the top-view picture, showing the grain structure of Ni_3Sn_4 . The results at the interface for the reaction between 37Pb-63Sn and Ni/Cu (experiment II) are quite similar to those of experiment I (Fig. 1a–d). The difference between these two sets of experiment is that, in experiment II, $(\text{Au}_{1-x}\text{Ni}_x)\text{Sn}_4$ particles did not exist because no Au layer was used.

The results became different when Cu was added to the solder (experiment III). In this case, no $(\text{Au}_{1-x}\text{Ni}_x)\text{Sn}_4$ particle was detected within the solder joint, and Ni_3Sn_4 was not present at the interface (Fig. 1e). An intermetallic compound with needlelike morphology was found at the interface (Fig. 1f). This compound was identified to be an Au-bearing $(\text{Cu}_{1-p-q}\text{Au}_p\text{Ni}_q)_6\text{Sn}_5$ compound with a Cu_6Sn_5 crystal structure. The evidence for the identification of this compound is presented below. The composition of this compound was $\text{Cu}_{0.47}\text{Au}_{0.02}\text{Ni}_{0.05}\text{Sn}_{0.46}$ (at.%) as determined using EPMA. The XRD result in Fig. 2 established that this compound was based on the Cu_6Sn_5 structure. In Fig. 2, the strong Ni peaks came from the Ni layer beneath the intermetallic compound. This result was further verified by TEM analysis, as shown in Fig. 3. It is worth noting that the long axis of the $(\text{Cu}_{1-p-q}\text{Au}_p\text{Ni}_q)_6\text{Sn}_5$ needle was along the c-axis of the hexagonal structure. In other words, the needle-shaped $(\text{Cu}_{1-p-q}\text{Au}_p\text{Ni}_q)_6\text{Sn}_5$ prefer to grow along the [0001] direction.

After Aging at 160°C for 0–2,000 H

After the reflow, solder joints were aged at 160°C for times ranging from 0 h to 2,000 h. Figure 4a–c

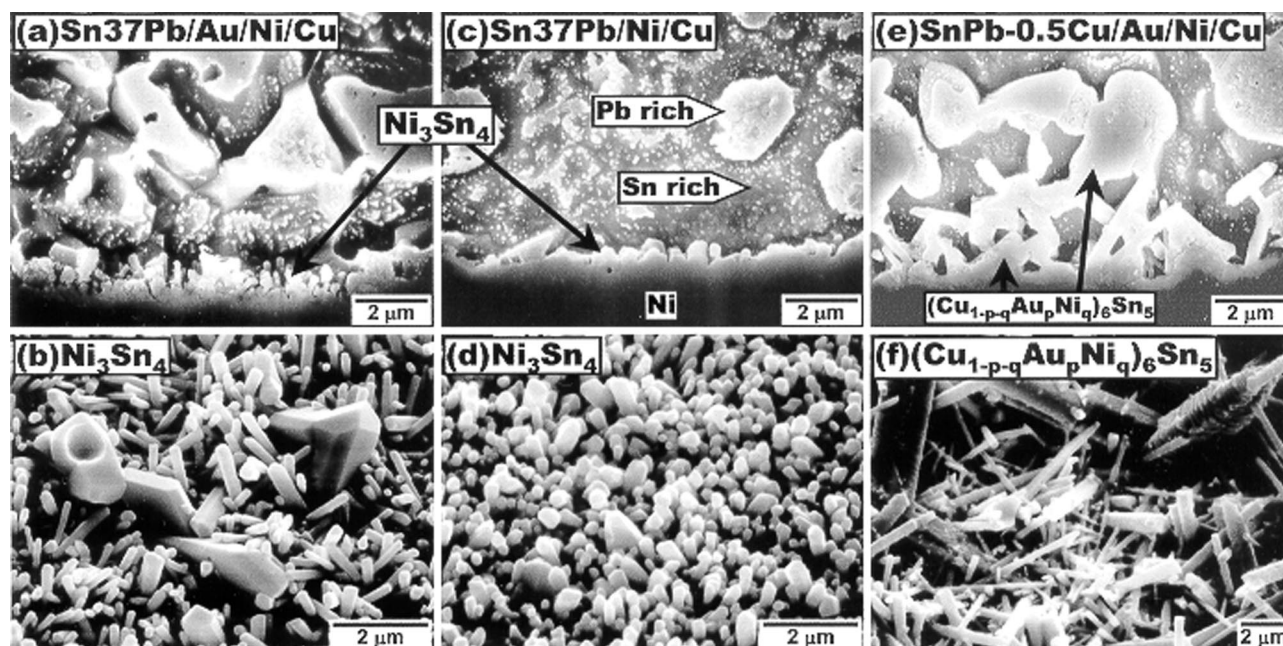


Fig. 1. (a) A cross-sectional view and (b) a top view of the reaction during reflow between 37Pb-63Sn and Au/Ni/Cu. A continuous layer of Ni_3Sn_4 formed at the interface. (c) A cross-sectional view and (d) a top view of the reaction during reflow between 37Pb-63Sn and Ni/Cu. A continuous layer of Ni_3Sn_4 formed at the interface. (e) A cross-sectional view and (f) a top view of the reaction during reflow between 36.8Pb-62.7Sn-0.5Cu and Au/Ni/Cu. A continuous layer of $(\text{Cu}_{1-p-q}\text{Au}_p\text{Ni}_q)_6\text{Sn}_5$ formed at the interface.

were the cross-sectional micrographs showing the interfaces that had been aged at 160°C for 2,000 h for experiments I, II, and III, respectively. Very different results were obtained for these three sets of experiments. In Fig. 4a (experiment I), a $14\text{-}\mu\text{m}$ layer of $(\text{Au}_{1-x}\text{Ni}_x)\text{Sn}_4$ and a $13\text{-}\mu\text{m}$ layer of Ni_3Sn_4 formed at the interface. The value of x for this $(\text{Au}_{1-x}\text{Ni}_x)\text{Sn}_4$ layer was determined by EPMA to be 0.55, which was greater than the x value for those $(\text{Au}_{1-x}\text{Ni}_x)\text{Sn}_4$ particles inside the solder joint before aging.^{2,3,8} According to XRD analysis, the compound $(\text{Au}_{0.45}\text{Ni}_{0.55})\text{Sn}_4$ has a orthorhombic structure, with the following lattice parameters: $a = 6.32 \text{ \AA}$, $b =$

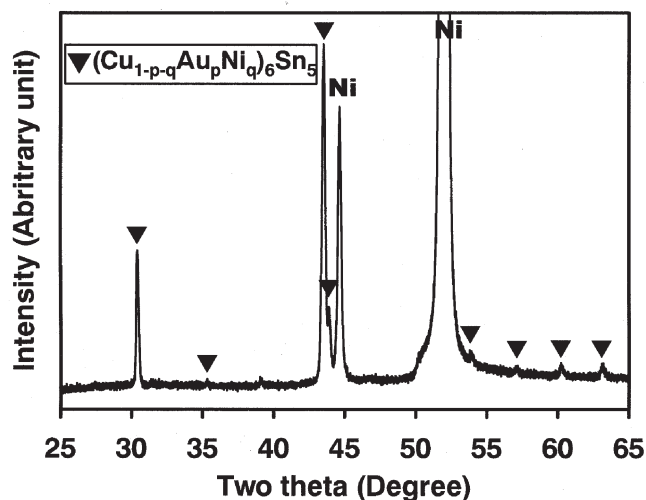


Fig. 2. The XRD pattern for the interface in Fig. 1f. This XRD result established that this compound is based on the Cu_6Sn_5 structure. The strong Ni peaks came from the Ni layer beneath the intermetallic compound.

6.39 \AA , and $c = 11.44 \text{ \AA}$. The driving force for $(\text{Au}_{1-x}\text{Ni}_x)\text{Sn}_4$ to regroup at the interface was to seek Ni at the interface to become more Ni rich.^{2,8} In Fig. 4a, the thickness of the Ni layer had been reduced from an initial value of $6.5 \text{ }\mu\text{m}$ (before reflow) to only $1.7 \text{ }\mu\text{m}$ after the 2,000-h aging. The nominal Ni consumption rate turns out to be $2.4 \times 10^{-3} \text{ }\mu\text{m}/(\text{h of aging})$ at 160°C , which is very close to the reported value of $2.8 \times 10^{-3} \text{ }\mu\text{m}/(\text{h of aging})$.² It should be noted that in calculating this nominal consumption rate those Ni consumed during reflow had been included.

In experiment II, the aging produced only a layer of Ni_3Sn_4 (Fig. 4b). The thickness of Ni_3Sn_4 was $9 \text{ }\mu\text{m}$, which is thinner than that in experiment I. The Ni thickness had been reduced from an initial value of $6.8 \text{ }\mu\text{m}$ (before reflow) to $4.4 \text{ }\mu\text{m}$, which was thicker than that in experiment I. The nominal consumption rate of Ni in experiment II was $1.2 \times 10^{-3} \text{ }\mu\text{m}/\text{h}$, which is less than half of the value of experiment I. This result shows that $(\text{Au}_{1-x}\text{Ni}_x)\text{Sn}_4$ not only lacked the ability as a diffusion barrier, but it also accelerated the growth of Ni_3Sn_4 .

Adding Cu into the solder produced very different results during aging (experiment III). As shown in Fig. 4c, only one layer of intermetallic existed. This layer was identified by EPMA to be $(\text{Cu}_{1-p-q}\text{Au}_p\text{Ni}_q)_6\text{Sn}_5$. The EPMA line scan (Fig. 5) showed that only $8\text{-}\mu\text{m}$ $(\text{Cu}_{1-p-q}\text{Au}_p\text{Ni}_q)_6\text{Sn}_5$ was detected at the interface. An obvious gradient of Ni concentration existed within the $(\text{Cu}_{1-p-q}\text{Au}_p\text{Ni}_q)_6\text{Sn}_5$ layer, suggesting that Ni is diffusing outward. In addition, the XRD analysis confirmed that this compound was based on the Cu_6Sn_5 crystal structure and had lattice parameters of $a = 4.23 \text{ \AA}$ and $c = 5.07 \text{ \AA}$. Inside

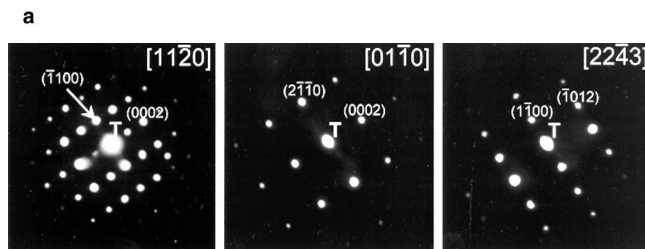
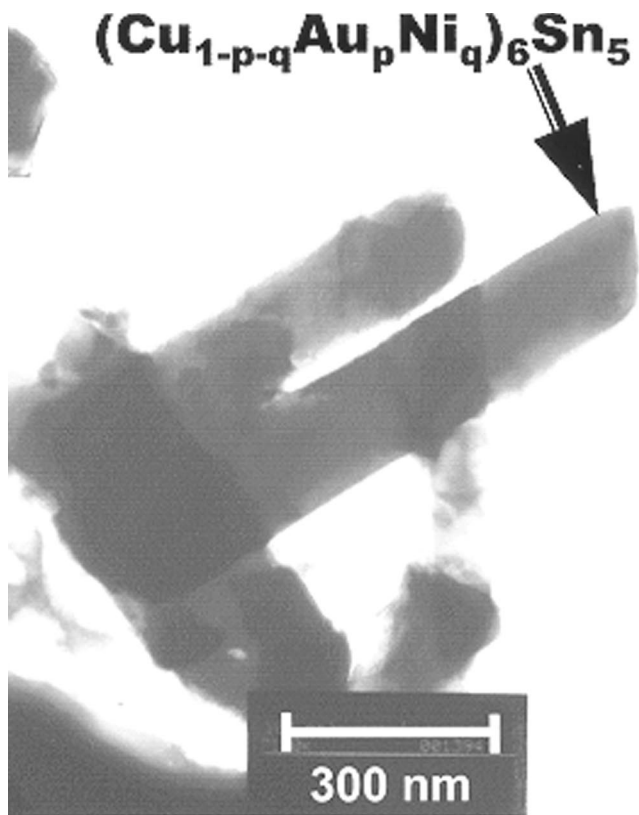


Fig. 3. (a) A TEM bright-field image for the $(\text{Cu}_{1-p-q}\text{Au}_p\text{Ni}_q)_6\text{Sn}_5$ compound. (b) The selected area diffraction patterns of $(\text{Cu}_{1-p-q}\text{Au}_p\text{Ni}_q)_6\text{Sn}_5$.

the solder, only a small amount of Cu_6Sn_5 -based particles, with lower Au and Ni concentrations compared to the compound at the interface, could be seen.

The most interesting aspect of experiment III is that the remaining Ni is much thicker compared to

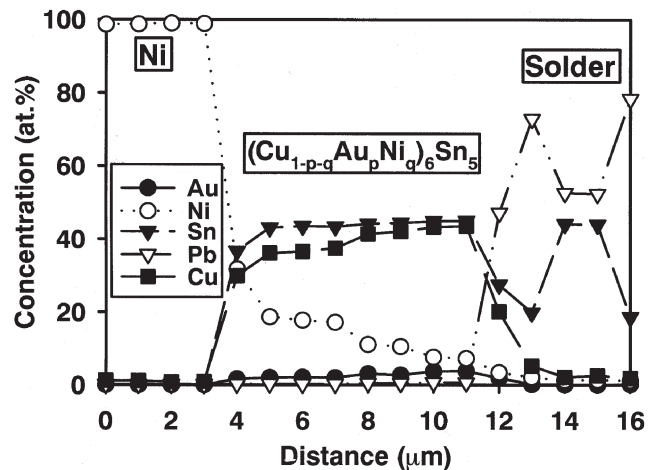


Fig. 5. An EPMA line scan across the reaction zone of the sample shown in Fig. 4c. Only one compound, $(\text{Cu}_{1-p-q}\text{Au}_p\text{Ni}_q)_6\text{Sn}_5$, was identified at the solder/Ni interface.

experiments I and II. As shown in Fig. 4c, after the 2,000-h aging, the Ni was still as thick as $7.1 \mu\text{m}$ (out of the original $7.7\text{-}\mu\text{m}$ Ni before reflow). This indicates that only a small amount of Ni was consumed when $(\text{Cu}_{1-p-q}\text{Au}_p\text{Ni}_q)_6\text{Sn}_5$ formed at the interface. The nominal Ni consumption rate was $2.8 \times 10^{-4} \mu\text{m}/\text{h}$. This value is one order of magnitude smaller than that of experiment I. In other words, doping solder with Cu can effectively reduce the consumption of Ni.

The growth kinetics data for experiments I, II, and III were summarized in Fig. 6. It can be seen that $(\text{Cu}_{0.70}\text{Au}_{0.05}\text{Ni}_{0.25})_6\text{Sn}_5$ grew slower than the growth of Ni_3Sn_4 in experiments I and II. Figure 6 also showed that $(\text{Au}_{1-x}\text{Ni}_x)\text{Sn}_4$ was not an effective diffusion barrier. It even accelerated the growth of Ni_3Sn_4 !

DISCUSSION

One major advantage of adding Cu into the solder is the ability of inhibiting the formation of the $(\text{Au}_{1-x}\text{Ni}_x)\text{Sn}_4$ layer at the interface during aging (Fig. 4a and c). The $(\text{Cu}_{1-p-q}\text{Au}_p\text{Ni}_q)_6\text{Sn}_5$ layer in Fig. 4c was also thinner compared to the overall thickness of $(\text{Au}_{1-x}\text{Ni}_x)\text{Sn}_4 + \text{Ni}_3\text{Sn}_4$ in Fig. 4a. Moreover, the formation of only $(\text{Cu}_{1-p-q}\text{Au}_p\text{Ni}_q)_6\text{Sn}_5$ could avoid the problematic $(\text{Au}_{1-x}\text{Ni}_x)\text{Sn}_4/\text{Ni}_3\text{Sn}_4$ inter-

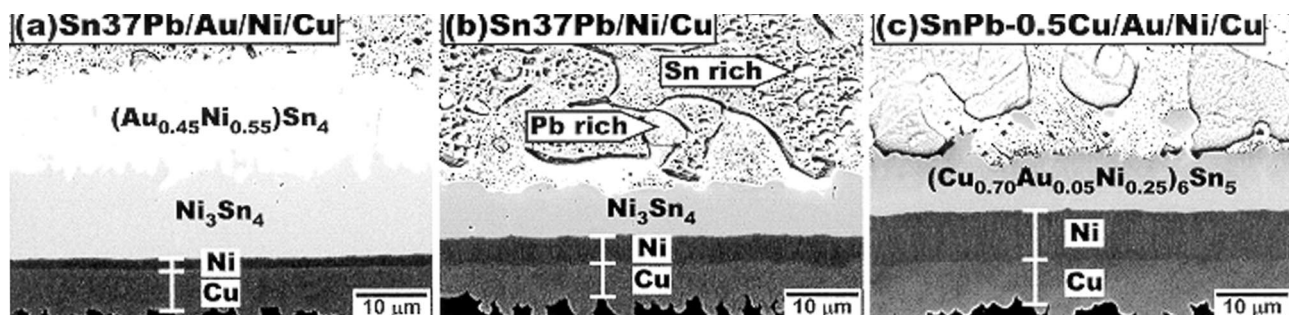


Fig. 4. (a) A cross-sectional micrograph for experiment I, which had been aged at 160°C for 2,000 h. A $14\text{-}\mu\text{m}$ layer of $(\text{Au}_{1-x}\text{Ni}_x)\text{Sn}_4$ layer and a $13\text{-}\mu\text{m}$ layer of Ni_3Sn_4 formed at the interface. (b) Same as (a) but for experiment II. Only a thinner Ni_3Sn_4 formed at the interface. (c) Same as (a) but for experiment III. A layer of $(\text{Cu}_{1-p-q}\text{Au}_p\text{Ni}_q)_6\text{Sn}_5$ formed at the interface.

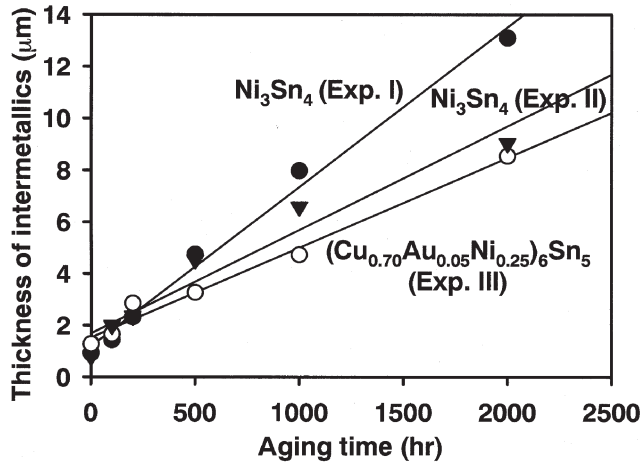


Fig. 6. The thickness of Ni_3Sn_4 (experiments I and II) and $(\text{Cu}_{0.70}\text{Au}_{0.05}\text{Ni}_{0.25})_6\text{Sn}_5$ (experiment III) versus time at 160°C .

metallic-to-intermetallic interface in experiment I. When Cu was added, the Au atoms were incorporated into $(\text{Cu}_{1-p-q}\text{Au}_p\text{Ni}_q)_6\text{Sn}_5$ and, consequently, $(\text{Au}_{1-x}\text{Ni}_x)\text{Sn}_4$ did not form.

The addition of Cu also reduced the Ni consumption. This reduction in Ni consumption suggests that a thinner Ni layer can be used for the Cu-doped solder joints. Considering the mass balance of Ni, the amount of Ni consumed is equal to the amount of Ni dissolved in the solder and the amount of Ni incorporated into the intermetallic compounds. The Ni contained in the intermetallic compounds includes Ni atoms in Ni_3Sn_4 , $(\text{Au}_{1-x}\text{Ni}_x)\text{Sn}_4$, and $(\text{Cu}_{1-p-q}\text{Au}_p\text{Ni}_q)_6\text{Sn}_5$. The intermetallic compounds can be separated into two groups: those inside the solder and those as continuous layers at the interface. The amount of the Ni-bearing intermetallics within a solder joint is relatively small and is ignored in our analysis.

The amount of Ni dissolved in the solder can be estimated by using the Ni-Pb-Sn phase diagram. According to the vertical section of the Ni eutectic-PbSn phase diagram,⁴ the solubility of Ni in eutectic PbSn is about 10^{-3} at.% at 220°C . The $750\text{-}\mu\text{m}$ solder balls used in this study had a mass of 2 mg, and the solder ball pads had a diameter of $600\text{ }\mu\text{m}$. At 220°C , a 2-mg solder ball can dissolve 8.4×10^{-6} mg Ni at saturation. This amount of Ni corresponds to a $0.0033\text{-}\mu\text{m}$ layer of Ni over a 600-mm soldering pad. This amount of Ni is quite small compared to the amount of Ni incorporated into the intermetallic compounds and can be ignored in the subsequent analysis. Therefore, it can be concluded that most of the consumed Ni was incorporated into the intermetallic compound layers at the interface.

Considering a fixed pad area, the thickness of Ni (d_{Ni}) consumed by forming the intermetallics at the interface is

$$d_{\text{Ni}} = \sum(d_{\text{IMC}_i} \times D_{\text{IMC}_i} \times W_{\text{IMC}_i})/D_{\text{Ni}} \quad (1)$$

where d_{IMC_i} is the thickness of the *i*th intermetallic compound at the interface, D_{IMC_i} is the density of

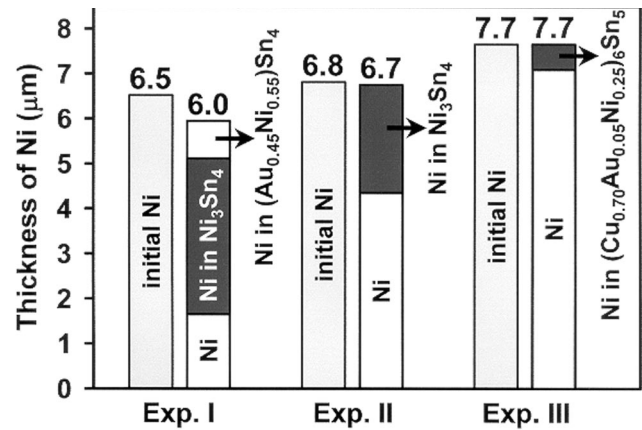


Fig. 7. A comparison of the original Ni thickness before reflow and the resulting distribution of Ni atoms after aging at 160°C for 2,000 h. The amounts of Ni atoms in the intermetallic compounds were expressed in term of pure Ni thickness.

the *i*th intermetallic, D_{Ni} is the Ni density, and W_{IMC_i} is the weight fraction of Ni in the *i*th intermetallic. From Eq. 1, it can be seen that the consumption of Ni by forming an intermetallic depends on the growth rate of the intermetallic and the Ni concentration in the intermetallic.

There are no literature values for the densities of Ni_3Sn_4 , $(\text{Au}_{0.45}\text{Ni}_{0.55})\text{Sn}_4$, Cu_6Sn_5 , or $(\text{Cu}_{0.70}\text{Au}_{0.05}\text{Ni}_{0.25})_6\text{Sn}_5$, but their theoretical values can be determined from their crystal structures, lattice constants, and atomic compositions. The lattice constants and the estimated theoretical densities for the Ni-bearing intermetallics are calculated and listed in Table I. Using Eq. 1, the data in Table I, and the thickness data for 2,000 h, the consumption of Ni by incorporation into intermetallics is calculated and plotted in Fig. 7. From the results of Fig. 7, it can be seen that the calculated values agree well with the original Ni thickness values before reflow. The data in Fig. 7 reveals that there are two reasons for experiment III to have a low Ni consumption. The first reason is that $(\text{Cu}_{0.70}\text{Au}_{0.05}\text{Ni}_{0.25})_6\text{Sn}_5$ had a lower growth rate and was an effective diffusion barrier. The second is that the Ni concentration in this compound was low, and the growth of this compound consumed little Ni.

In industrial applications, the source of Cu does not have to be limited to the Cu added into the solder on purpose. The Cu atoms can actually come from the dissolution of the Cu layer from the other side of the solder joints. One example of such a situation occurs in soldering BGA packages to printed circuit boards. In this case, the soldering pads on the BGA packages have the Au/Ni/Cu surface finish, and the printed circuit boards have the OSP/Cu surface finish. After reflow, the OSP disappears from the interface, and the Cu is then exposed to the solder and supplies Cu into the solder joints. Similar situation can also occur in low-cost flip-chip packages, where Au/Ni metallization is used.

Table I. The Lattice Parameters and the Estimated Theoretical Densities for Ni_3Sn_4 , AuSn_4 , $(\text{Au}_{0.45}\text{Ni}_{0.55})\text{Sn}_4$, Cu_6Sn_5 , and $(\text{Cu}_{0.70}\text{Au}_{0.05}\text{Ni}_{0.25})_6\text{Sn}_5$

Phase	Lattice Parameters (Å)	References	Estimated Theoretical Density (g/cm^3)
Ni*	a = 3.5350	13	8.9
Ni_3Sn_4	a = 12.3712 b = 4.06096 c = 5.21007 $\beta = 104.061^\circ$	14, 15	8.5
AuSn_4	a = 6.51241 b = 6.51621 c = 11.70651	3, 16	9.0
$(\text{Au}_{0.45}\text{Ni}_{0.55})\text{Sn}_4$	a = 6.32 b = 6.39 c = 11.44	17	8.6
Cu_6Sn_5	a = 4.1922 c = 5.0372	18	7.9
$(\text{Cu}_{0.70}\text{Au}_{0.05}\text{Ni}_{0.25})_6\text{Sn}_5$	a = 4.23 c = 5.07	This study	8.0

*Data for Ni are all literature values and are listed for reference.

CONCLUSIONS

This study pointed out that adding Cu into solder had two advantages. The first advantage was that adding Cu completely inhibited the deposition of the $(\text{Au}_{1-x}\text{Ni}_x)\text{Sn}_4$ layer. Only a layer of $(\text{Cu}_{1-p-q}\text{Au}_p\text{Ni}_q)_6\text{Sn}_5$ formed at the interface of the Cu-doped solder joints. The formation of only $(\text{Cu}_{1-p-q}\text{Au}_p\text{Ni}_q)_6\text{Sn}_5$ avoided the problematic $(\text{Au}_{1-x}\text{Ni}_x)\text{Sn}_4/\text{Ni}_3\text{Sn}_4$ intermetallic-to-intermetallic interface.

The second advantage was that the formation of $(\text{Cu}_{1-p-q}\text{Au}_p\text{Ni}_q)_6\text{Sn}_5$ significantly reduced the consumption rate of the Ni layer. This reduction in Ni consumption allows a thinner Ni layer to be used in Cu-doped solder joints. There were two reasons for the low Ni consumption. The first reason was that $(\text{Cu}_{0.70}\text{Au}_{0.05}\text{Ni}_{0.25})_6\text{Sn}_5$ had a lower growth rate and was an effective diffusion barrier. The second reason was that the Ni concentration in this compound was low compared to Ni_3Sn_4 , and therefore, the growth of this compound consumed little Ni.

ACKNOWLEDGEMENTS

The authors thank the National Science Council of Republic of China for the financial support of this study through Grant Nos. NSC-90-2216-E-008-009 and NSC-90-2214-E-008-007. The authors also thank Mei-Li Cheng (NCTU, TEM analysis) and Chung-Yuan Kao, His-Chuan Lu, and Hsiao-Jen Chen (NTU, EPMA analysis) for their assistance in conducting this research.

REFERENCES

1. K.N. Tu and K. Zeng, *Mater. Sci. Eng.* R34, 1 (2001).
2. C.E. Ho, W.T. Chen, and C.R. Kao, *J. Electron. Mater.* 30, 379 (2001).
3. C.E. Ho, Y.M. Chen, and C.R. Kao, *J. Electron. Mater.* 28, 1231 (1999).
4. K. Kulojärvi, V. Vuorinen, and J.K. Vilahti, *Microelectron. Int.* 15, 20 (1998).
5. Z. Mei, M. Kaufmann, A. Eslambolchi, and P. Johnson, *1998 IEEE Electronic Components and Technology Conference Proceedings* (Piscataway, NJ: IEEE, 1998), p. 952.
6. A. Zribi, R.R. Chromik, R. Presthus, J. Clum, K. Teed, L. Zavali, J. DeVita, J. Tova, and E. J. Cotts, *1999 IEEE Electronic Components and Technology Conference Proceedings* (Piscataway, NJ: IEEE, 1999), p. 451.
7. A. Zribi et al., *2000 IEEE Electron. Comp. Technol. Conf. Proc.* (Piscataway, NJ: IEEE, 2000), p. 383.
8. C.E. Ho, R. Zheng, G.L. Luo, A.H. Lin, and C.R. Kao, *J. Electron. Mater.* 29, 1175 (2000).
9. A.M. Minor and J.W. Morris, Jr., *Metall. Mater. Trans. A* 31, 798 (2000).
10. A.M. Minor and J.W. Morris, Jr., *J. Electron. Mater.* 29, 1170 (2000).
11. C.R. Kao and C.E. Ho, Republic of China patent 149096I (23 March 2001).
12. J.H. Lee, J.H. Park, Y.H. Lee, and Y.S. Kim, *J. Mater. Res.* 16, 1249 (2001).
13. M. Yousuf, P.C. Sahu, H.K. Rajagopalan, and K.G. Rajan, *J. Phys. F: Met. Phys.* 16F, 373 (1986).
14. H. Nowotny and K. Schubert, *Z. Metallkd.* 37, 23 (1946).
15. S. Furuseth and H. Fjellvag, *Acta Chem. Scand. Ser. A: Phys. Inorg. Chem.* 40A, 695 (1986).
16. R. Kubiak, *J. Less-Common Met.* 80, 53 (1981).
17. C.E. Ho, W.T. Chen, R.Y. Tsai, and C.R. Kao, unpublished research.
18. A. Ganguluee, G.C. Das, and M.B. Bever, *Metall. Trans.* 4, 2063 (1973).